Journal of Mining and Earth Sciences

Stability conditions of jointed rock slope with contact dynamics method

Tuan Anh Nguyen[*]

Faculty of Mining, Hanoi University of Mining and Geology, Vietnam

ARTICLE INFO

ABSTRACT

This paper proposes the modeling of the contact dynamics as a non-smooth discrete element method (NSCD). The theoretical basis of a new approach which makes it possible to consider a better surface contact with friction between polyhedric discrete elements simultaneously is studied. The results of the application of the NSCD to investigate the verified examples present the stability conditions of jointed rock slopes. The rock mass is first geometrically represented through the distribution of discontinuities in the rock mass and the use of the LMGC90 code based on the discrete fracture network (DFN) method. The 3D computational models are analysed by using the LMGC90 based on the NSCD method. The application of the methodology of numerical simulation of multi-phase excavation of rock slope cut is provided. A case study of the data was performed on the benches of a limestone clues quarry situated in the south of France. The mechanical responses of the numerical rock mass are analysed and evaluated.

1. Introduction

Discrete elements method as polydedron in numerical simulation was developed by (Cundall and Strack, 1979). In this paper, the algorithm of the general resolution used in the non-smooth contact dynamics (NSCD) method, and developed in the laboratory LMGC with the works (Jean, 1999). Non-smooth dynamics in contact frame is based on a node by node resolution of the contact. The laws of Signorini for unilateral contact and of Coulomb for friction are not regularized (Dubois and Jean, 2006; Radjai and Richefeu, 2009). The NSCD method is distinguishable from the original smooth DEM due to the following features: An implicit scheme for intergrating the time discretized dynamical equation; A non-regularized interaction law (Signorini unilateral contact and Coulomb dry friction); The possiblility for finite element discretzation in order to take into account the mechanical behaviour of rock blocks.

Corresponding author
E-mail: nguyenanhtuan@humg.edu.vn

2. Non-smooth contact dynamics method

2.1. Introduction

The NSCD method is relies on a special formulation of the mathematical and mechanical background allowing us to deal with some extended kinds of laws (coulomb friction, shock law). For the non-smooth in time, the occurrence of velocity jumps is a well know feature of the second order dynamics with unilateral constraints on the position even with continuous media.

The contact forces between two bodies are bound by the principle of mutual actions. At any time of the evoluation of the system one needs to define the interaction locals and an associated local frame in order to describe the interaction behavior.

It is assumed that one is able to define for each point (C) of the "candidate" boundary and its (unique) nearest point (A) on the "antagonist" boundary. It allows us to define for each couple of points a local frame (t, n, s) with n the normal vector of the antagonist boundary and (s, t) two vectors of its tangential plane is determined.
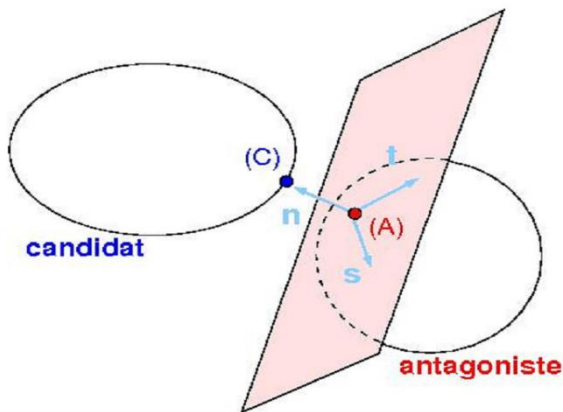

Figure 1. A potential contact between two particles

The calcultation of contact forces in the NSCD method is performed in two steps.

In the first step, the result of the interaction of the antagonist body (A) on the candidate body (C) can be considered to be equal to the force r_α acting at the contac point beween these two bodies. At the contact α, the normal vector n_α pointing from antagonist to candidate body two tangential vectors and, which define the tangential space by respecting this convention $s_\alpha \times t_\alpha = n_\alpha$. On other hand, we denote the gap distance between bodies along the normal direction. This value will be negative if there is an interpenetration between the bodies.

In the second step, by the definition of a linear mapping H_α, that relates the local forces to the global forces, verifying the lolling equation:

$$R_\alpha = H_\alpha(q)\, r_\alpha \qquad (1)$$

where $H_\alpha(q)$ is a mapping which contains the local information about contactors.

Finally, the global contacs forces can be obtained by the relation:

$$R = \sum_\alpha R_\alpha \qquad (2)$$

The same procedure is employed for the velocity calculation and the velocity of the bodies can be expressed in the local frame.

The contact conditions are solved at the local level; the impulse force is R and the relative velocity U. The dynamic equations are solved at the global level with an algorithm of the NSCD method. The global impulse force is noted r and the global velocity vector is noted. H and H* are the mapping operators to pass from local to global unknowns (Jean, 1999; Mereau, 1998; Dubois, 2011), as shown in Figure 2.
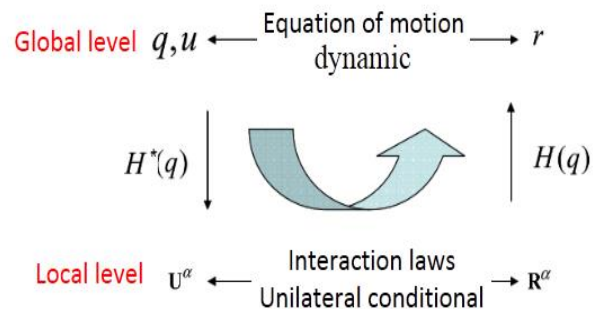

Figure 2. Algorithm of the NSCD method

The NSCD method is distinguishable from the smooth DEM due to the following features: an implicit schema for integrating the time discretized dynamical equation; a non-regularized interaction law (Signorini condition

and contact law of Coulomb). The code Lmgc90 is a general-purpose open-source software developed at LMGC Laboratory of Montpellier II, capable of modeling an extensive collection of deformable or undeformable particles of various shapes, with different interaction laws. Lmgc90 declares the mechanical models of DFN and the contact behavior in the discontinuities. The models of fractured rock mass on Lmgc90 for the simulation and analysis under the NSCD method, for detailed explanation in (Dubois and Jean, 2006; Radjai and Richefeu, 2009).

In these many choices, the NSCD method is used punctual contact with extended law (transmission of torque); multi-punctual contacts with classical interaction laws; continuous surfaced description. Less trivial in usual cases: not strictly convex (cubes, bricks); only locally convex (general polydedron, triangulated surface); not convex at all, it may be decomposed in not strictly convex shapes. Only in simplest cases (rigid body with strictly convex boundary) the interaction locus maybe considered as punctual.

Collision detection is a huge problem. The most popular approach is defining a contact force R = k*g at each contact point where k is a stiffness and g is a measure of the interpenetration between a pair of objects. The value k depends on the nature of the objects, the type of interaction, and other elements of the simulation. No matter how k is chosen. Hence, when g is negative which generates force. g is positive when the objects are no longer in contact.

2.2. Signorini condition

The NSCD of objects in contact has been extensively studied in the mechanical simulation of a jointed rock mass in contact. A contradiction with Signorini's condition of contact shown in Figure. 5a at the point of contact, there exists a complementarity relation between the interpenetration distance g and normal contact force R_N as such in Equation (3).

$$R_N \geq 0; \ g \geq 0; \ R_N * g = 0 \qquad (3)$$

where g is the algebraic distance between two bodies at the point of contact and R_N is the amplitude of normal force needed to solve the contacts. In the case of frictional sliding, a tangential component R_T is introduced, leading to a contact force $R = (R_N, R_T)$. For the dynamical problem, it is more natural to formulate the unilateral contact in term of velocities with assuming $g(t_o) \geq 0$ then $\forall t > t_o$ if $g(t) \leq 0$ then $U_N \geq 0$, $R_N \geq 0$, $U_N * R_N = 0$ else $R_N = 0$.
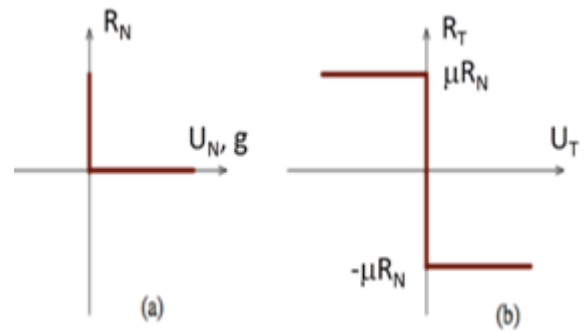

Figure 5. The relation curve of the contact in NSCD method: (a) Signorini condition and (b) Coulomb contact law

2.3. Contact law of Coulomb

Following the Coulomb contact law shown in Figure 5b, the sliding at the contact point only appears when the tangential component of the contact forces between two objects is large than the sliding threshold. This condition is given as

$$\begin{cases} g = 0 \rightarrow |R_T| \leq \mu \, R_N \rightarrow \text{nonsliding} \rightarrow U_T = 0 \\ U_T < 0 \rightarrow R_T = \mu \, R_N \rightarrow \text{sliding towards the back} \\ U_T > 0 \rightarrow R_T = -\mu \, R_N \rightarrow \text{sliding forwards} \end{cases} \quad (4)$$

where $U = (U_N, U_T)$ is the sliding velocity vector between two objects, $\mu = \tan(\varphi)$ is friction coefficient and φ is the internal friction angle. It is existed a parameter $\rho > 0$ that $U_T = -\rho . R_T$ with frictional contact (Signorini-Coulomb).

3. Verification examples

The block on an inclined surface used to test the model is a rigid block sliding on an inclined plane as depicted in Figure.6. In the case of the block on an inclined, the actions of contact are considered localized at points A and

B which assumed to always remain in dry contact with friction, on a tilted plane and subjected to its weight P applied to the centre of inertia. We have three equations and unknown nodal forces. Assuming that the solids are rigid, the sliding can only take place simultaneously at two ends A and B of the segment. We have a nonlinear problem to be solved, of four equations for four unknown variables. This method of modeling can be applied in 3D to the case of the contact (contact of convex) of an edge of a polyhedron with a plane surface. The case of the linear contact can be reduced to the 2D case, in the plane of contact.

The unit depth rectangular block of length b and height a lies on an inclined surface with a slope angle β. The friction angle between the block and the inclined surface is specified through the joint friction angle φ. The aspect ratio of the block and orientation was chosen such that the mode of failure is sliding. The block on the inclined plane will accelerate down the plane. The block acceleration is determined by acceleration due to gravity (g), the slope angle (β), and the angle of friction (φ). The analytical solution for the displacement of the block centroid due to gravity is estimated.
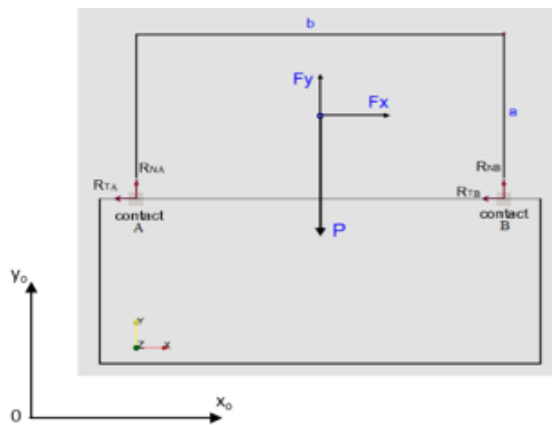

Figure 6. Hypothesis of the distribution of the tangential actions in a direction

The assumptions about normal and tangential actions providing the possibility to avoid the indetermination in the case of plane contact are comprehensively explained by (Bohatier and Vinches, 2007). The contact force in each node is composed of normal and tangential forces.

Here the hypothesis of a linear distribution of the tangential action is presented, with its mechanical consequences. For a 2D problem, we can write for the dependency of the tangential forces at A and B vertices shown in Figure 6 in a polygonal contact surface with regard to the normal forces.

$$\frac{R_{TA}}{R_{NA}} = \frac{R_{TB}}{R_{NB}} \tag{5}$$

R_{TA} and R_{TB} are the tangential forces R_{NA} and R_{NB} are the positive normal forces.

Conditions of adherence of two nodes as
Relation along x: $R_{TA} + R_{TB} + F_x = 0$
Relation along y: $R_{NA} + R_{NB} + F_y = 0$ $\tag{6}$
Equilibrating of the normal and tangential actions at A and B vertices.

$$-(R_{TA} + R_{TB})\frac{a}{2} + (R_{NA} - R_{NB})\frac{b}{2} = 0 \tag{8}$$

Contact force on each node is composed for normal and tangential forces at points A and B:

$$R_{NA} = -\frac{a}{2b}F_x - \frac{F_y}{2}; \ R_{NB} = \frac{a}{2b}F_x - \frac{F_y}{2} \tag{9}$$

$$R_{TA} = \frac{F_x \cdot \left(F_x \cdot \frac{a}{b} + F_y\right)}{2 \cdot F_y}; \ R_{TB} = \frac{F_x \cdot \left(F_y - F_x \cdot \frac{a}{b}\right)}{2 \cdot F} \tag{10}$$

The sliding conditions with the regard to the Coulomb friction laws occur along AB

$$T = P*\mu \tag{11}$$

where P = m*g, m is the mass of block; μ is the friction coefficient. For the other motion: RNA=RNB=-(m*g)/2; and for example, C = 0 Pa, μ=0.577 and a = 0.5 m, b = 1 m.

The proposed assumption (5) is compatible with the sliding conditions with regard to the Coulomb friction law and the equiprojectivity property of the velocity field onto the contact. with problem geometry in the Figure 7, the block is analytically on the Table 1.

For generalization to 3D problem, as first step a plane contact on a triangular surface can be considered, with the actions of contact located at its certices (Perales, 2007). After writing the Equation (5) for each edge of the triangle,

Table 1. The contact force on each node at A and B vertices

Case	β°	f=tan(β)	Fx, N	Fy, N	R_{NA}, N	R_{NB}, N	R_{TA}, N	R_{TB}, N
Adherence	0	0	0	-12262.50	6131.25	6131.25	0	0
	10	0.1763	2129.36	-12076.21	5505.76	6570.44	-1158.55	-970.81
	30	0.5774	6131.25	-10619.64	3777.01	6842.63	-3950.59	-2180.66
Sliding	40	0.8391	5423.41	-9393.62	3340.96	6052.66	-3494.51	-1928.90

it is possible to verify that these relations are compatible with the various situations including three nodes slide, a node is fixed with conditions of adherence and two nodes do not slide in which case the third node necessarily does not slide.

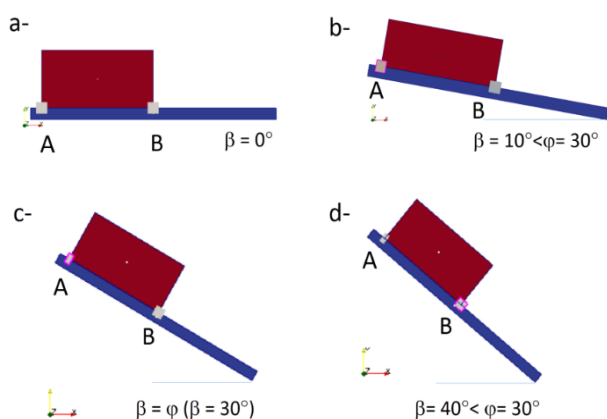Finally, a contact algorithm starts by the valuation of a sticking contact where the

Figure 7. Block sliding on inclined surface

assumption (5) is taken into account. When a nodal contact force is greater than the authorized value by Coulomb's law, it is limited. Then its direction is used to determine the sliding velocity. When the solid slides on a triangular surface, the set of 6 dynamic equations for one solid is consistent to determine the normal nodal contact force with three nodal contact points. When there are more than three nodal contact points the linear spatial dependency of normal forces and two tangential equations which given by the supplementary nodes provides the extra equations for the solution.

The block on the inclined plane will accelerate down the plane. The block

acceleration is determined by acceleration due to gravity (g): P=m*g =12262,5N and m = a*b*γ (γ=2500kg/m3, unit weight) of the block centroid due to gravity. Hence, Fy = P*cosβ; and Fx = Fy*tanφ with β > φ or Fx = Fy*tanβ with β < φ.

Application on LMGC90 with case adherence β = 0° is shown in Figure 7a, β = 10°<φ= 30°, as shown in Figure 7b, β = φ (β = 30°), as shown in Figure 7c, and β = 40°< φ = 30°, as shown in Figure 7d which are verifed.

When the calculation converge with the step of time dt=0.01 sec.: RTA=RTB=0 and RNA=RNB = 6131.25, N with β = 0°and φ = 30° shown in Figure 8a; β = 10°and φ = 30° shown in Figure 8b; β = φ (β = 30°) Shown in Figure 8c; β = 40° and φ = 30° with RT/RN = μ = tanφ is shown in Figure 8d as a function of time.

4. Numerical results using the NSCD method

In this case, we have 61 discontinuities and stratification on 9 benches from the Clues quarry. This quarry of the Grave de Blausacs (06) is situated in France 20km north of Nice. The studied slope is excavated in the quarry, and the cut has an average benches height of 15m with a slope of 70°. The grouping of discontinuities into 4 mains familes is based on their genesis and orientation.

In the studied quarry, a significant cohesion exists, because no important block fall was mentioned but using no cohesion allows depicting the influence of the grouping on failure. The limit equilibrium stability method analysis is used for its rapidity allowing to obtain results, but stress-strain computation using LMGC90 in this case.

Figure 10 shows the static results for the excavation procedure with the NSCD method in LMGC90. Jointed rock mass modeling deals with an application of rock mechanics with the case 3D and 2D model, as shown in Figure 11. The models created from the first and the third combinations were chosen to be applied in our simulation. The future slope modelling was simulated and assigned following the excavation procedure: preparation phase; 1 excavation phase; 2 excavation phase; 3 finishing phase.
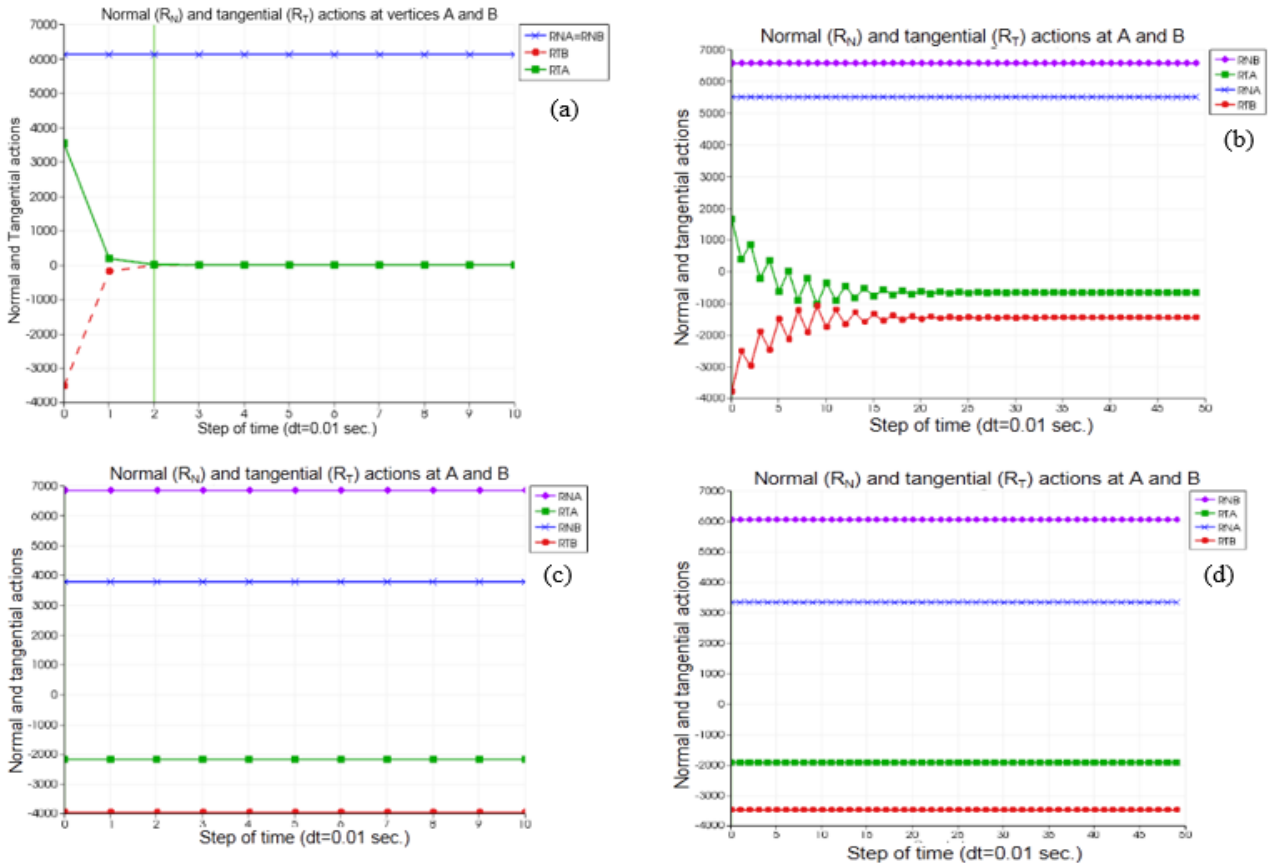

Figure 8. The assumptions about normal and tangential actions of block on inclined surface with case: β = 0°and φ = 30° (a); β = 10°and φ = 30° (b); β = φ = 30°(c); β = 40° and φ = 30° with $R_T/R_N = \mu = \tan\varphi$ (d) as a function of the time.
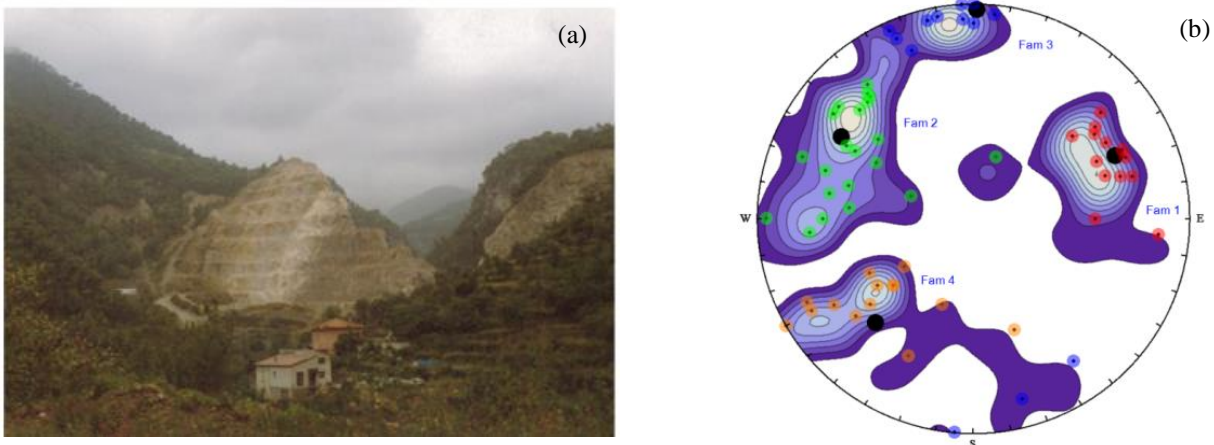

Figure 9. Photo of the Clues quarry (a) and stereographic projection, in 4 mains families with spectral method and density plot (b) (Nguyen et al., 2014).

a- state 1
The total rock mass without the excavation

b- state 2
The rock mass that is 1st excavation phase (1)

c- state 3
The rock mass that is 2st excavation phase (2)

d- state 4
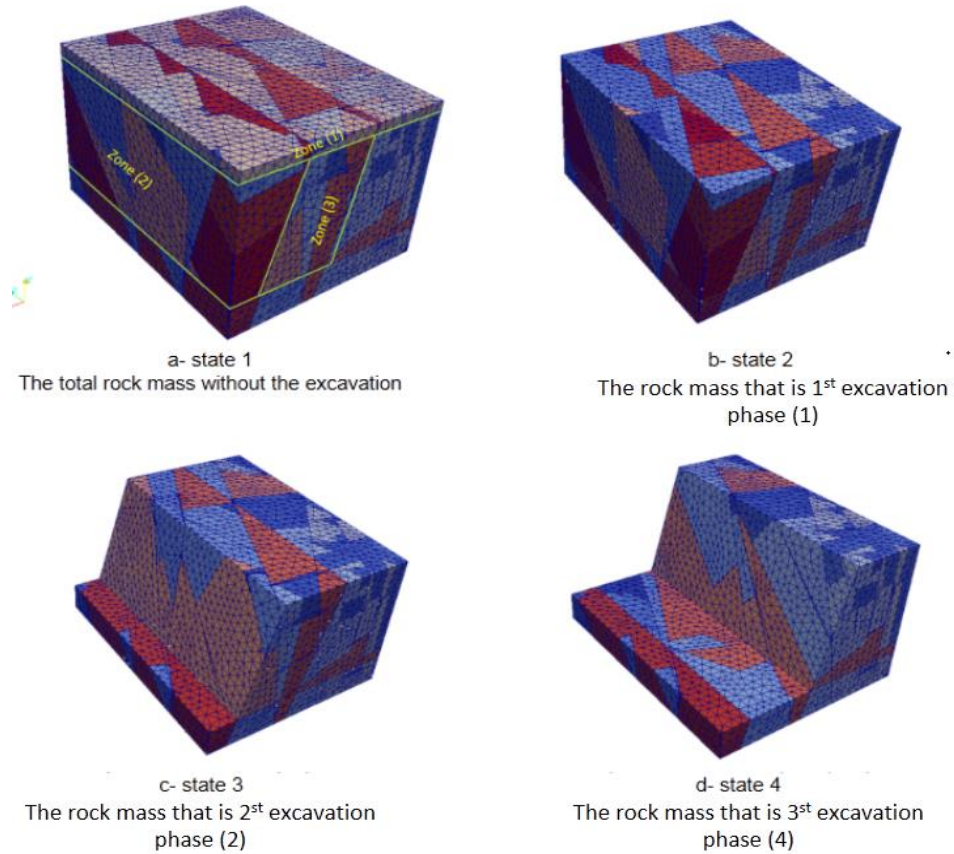The rock mass that is 3st excavation phase (4)

Figure 10. Numerical rock mass before and after the slope cutting, the model rock mass during the excavation procedure: a- preparation phase; b- 1 excavation phase; c- 2 excavation phase; d- 3 finishing phase. Four discotninuities sets using the colour signify: one colour/set
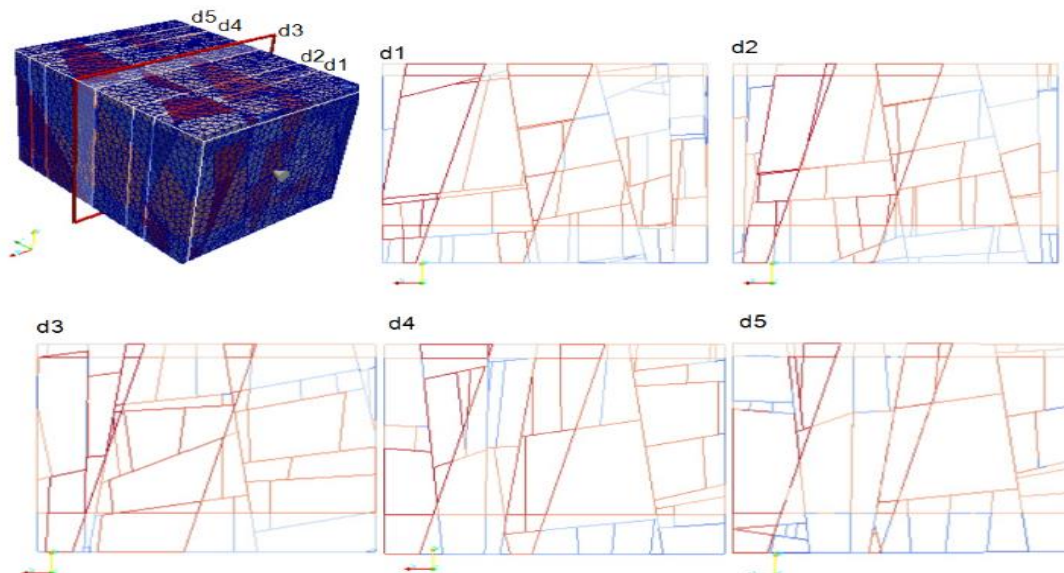

Figure 11. Model (2D) of a rock mass subjected for slope stability analysis purpose from model (3D), (Nguyen et al., 2014; Nguyen et al., 2015)

Two stability critical for the whole rock masse were applied for the simulation during the excavation procedure: all rock blocks must not displace outside a limited zone of 25x25x50 m which is 2.5 times larger than the initial rock mass and the velocity tolerance of all rock blocks must not be excess the predicted limit of 1 m/s.

The correlation of the contact parameters of model was studied and presented on the graphs of time versus the number of the contacts, shown in Figure 12; and the velocity of block unstable in the model, shown in Figure 13. There are 4 blocks with the total volume of the unstable block 21,078 m^3 in the state 3 is 2st excavation phase shown in Figure 14.
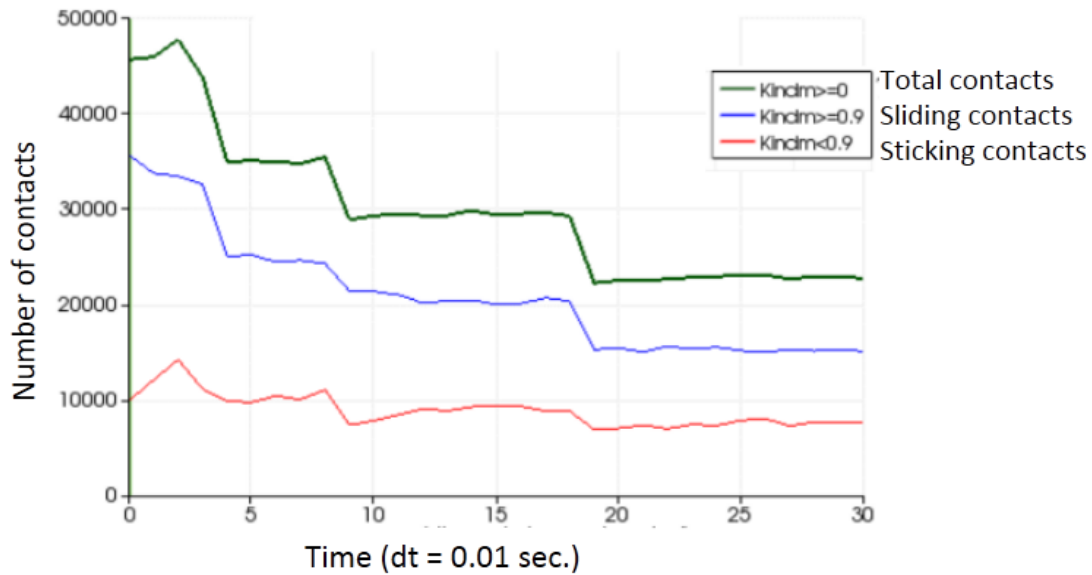

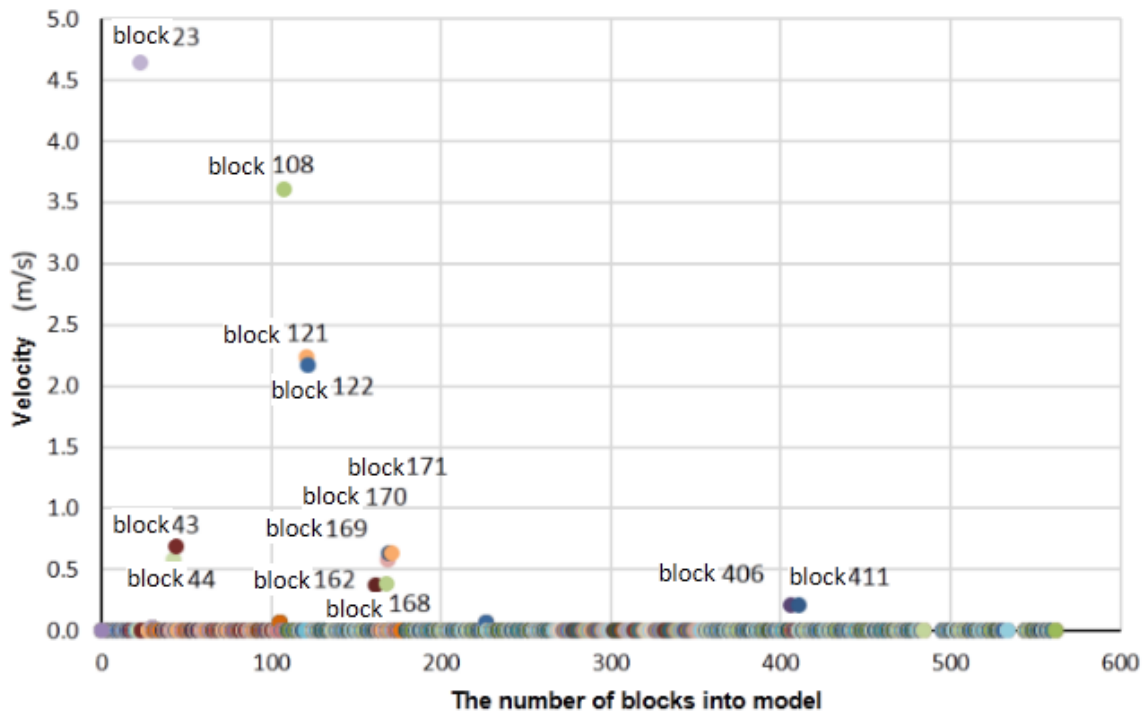*Figure 12. Correlation of contact parameters into the model*

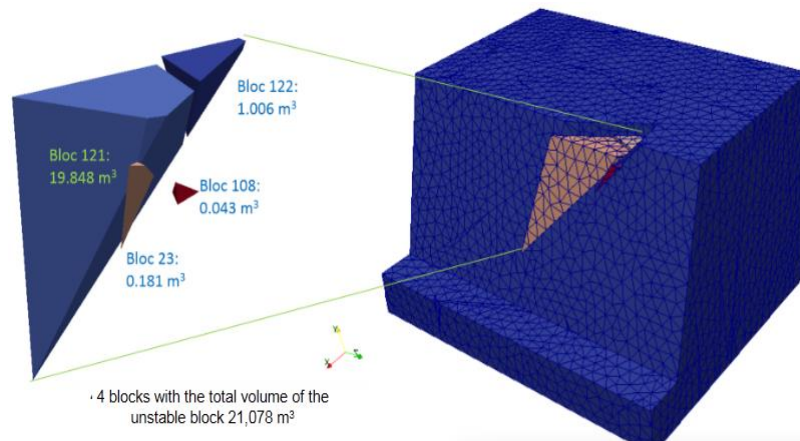*Figure 13 Correlation of the velocity versus the number of the unstable block into model*

Fiaure 14. The number of unstable blocks in the state 3 is 2ˢᵗ

5. Conclusion

The NSCD method approach relies on a NLGS algorithm into LMGC90. Considering, one by one, the local systems to solve for each contact α was determined. To verify the model, it is necessary to demonstrate that the solution it produces agrees within an acceptale margin of error with independent solution to the problem. The independent solution can be based on laboratory test cases, physical models, field case studies or an analytical solution.

The contact dynamics method approach based on a joint model developed in this paper has been successfully in the LMGC90 software. Verification examples demonstrats that the new NSCD model is able to model the behavior of a jointed rock mass and produce results with good accuracacy comared to analytical solutions and DEM.

In this paper, a new model is proposed for the plane contact, based on the spatial dependency of the tangential forces with regards to the normal forces by the NSCD method. Then, a jointed rock mass model is provided for application to rock mechanics with a reduction of computation time.

Acknowledgement

References

Cundall, P. A. and Strack, O.D.L., 1979. Discrete numerical model for granular assemblies. *Geotechnique* 29(1), 47–65.

Dubois, F. and Jean, M., 2006. The non smooth contact dynamic method: recent LMGC90 software developments and application. *Analysis and Simulation of Contact Problems*. Springer Berlin Heidelberg.

Jean, M., 1999. The non-smooth contact dynamics method. *Computer Methods in Applied Mechanics and Engineering* 177(3-4), 235-257.

Nguyen, A.T., Merrien-Soukatchoff, V. and Vinches, M., 2014. Grouping discontinuities of fractured rock mass into main sets: consequences on the stability analysis of open pit benches. *Bulletin of Engineering Geology and the Environment*, Springer Berlin Heidelberg, 17-29.

Nguyen, A.T., Merrien-Soukatchoff, V., Vinches, M., Gasc-Barbier, M., 2015. Grouping discontinuities in representative sets: influence on the stability analysis of slope cuts. *Bulletin of Engineering Geology and the Environment*, Springer Berlin Heidelberg, 1429-1444.

Radjai, F. and Richefeu, V., 2009. Contact dynamics as a nonsmooth discrete element method. *Mechanics of Materials* 41(6), 715-728.